Immunity, Volume

Supplemental Information

The Xenobiotic Transporter Mdr1 Permits T Cell Adaptation to Bile Acid Reabsorption in the Ileum

Wei Cao, Hisako Kayama, Mei Lan Chen, Amber Delmas, Amy Sun, Sang Yong Kim, Erumbi S. Rangarajan, Kelly McKevitt, Amanda P. Beck, Cody B. Jackson, Gogce Crynen, Angelos Oikonomopoulos, Precious N. Lacey, Gustavo J. Martinez, Tina Izard, Robin G. Lorenz, Alex Rodriguez-Palacios, Fabio Cominelli, Maria T. Abreu Daniel W. Hommes, Sergei B. Koralov, Kiyoshi Takeda, and Mark S. Sundrud

SUPPLEMENTAL FIGURES

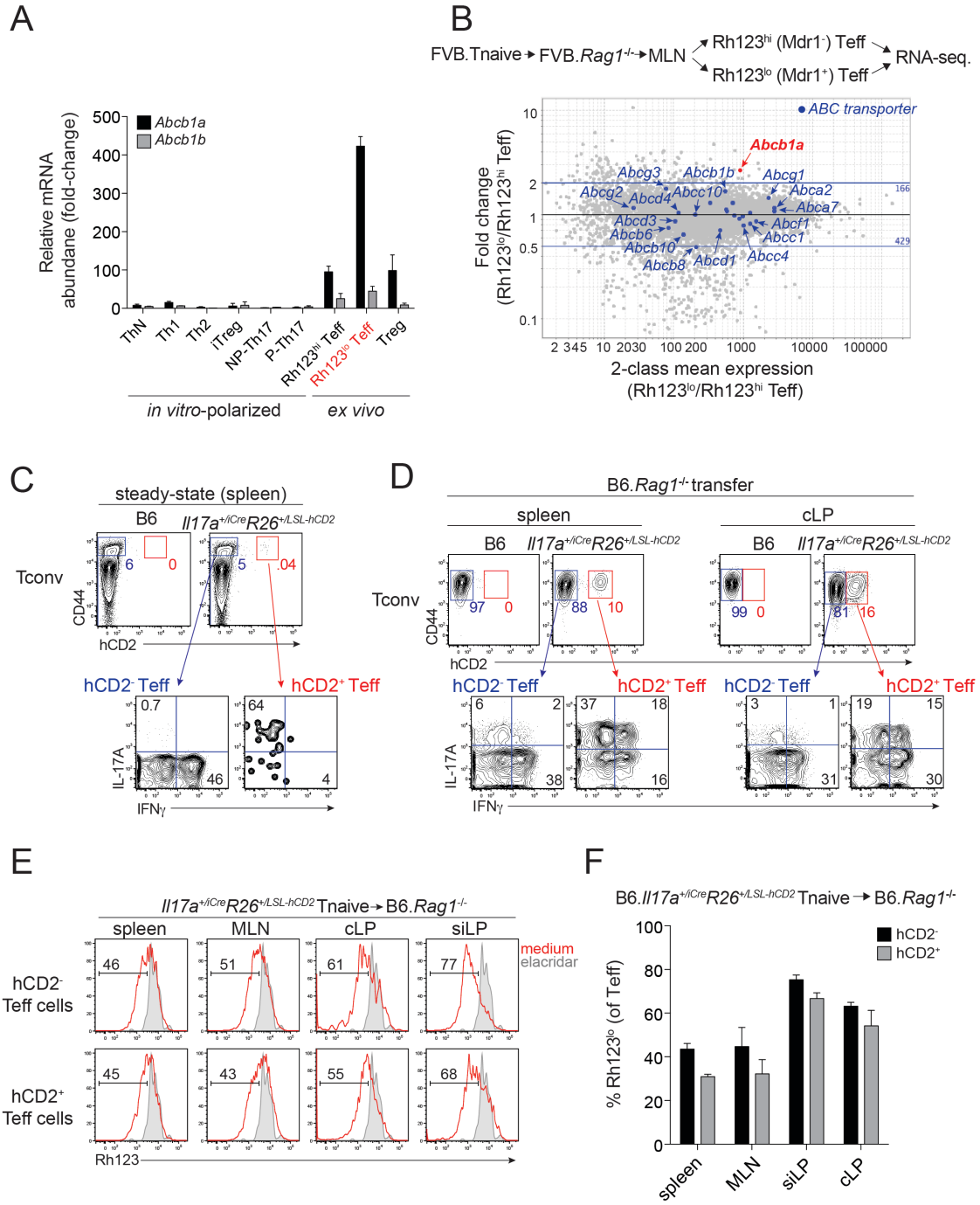

Figure S1. Rh123 efflux is a Specific Measure of Mdr1 Expression in Mouse CD4$^+$ Effector T Cells and is Expressed in Intestinal Th17 and Th1 Subsets (related to Figure 1).

(A) Mean fold-change in abundance of Mdr1 mRNAs (*Abcb1a*, *Abcb1b*) (± SEM; n = 3), determined by nanostring, in *in vitro*-polarized or *ex vivo*-isolated wild type (B6) CD4$^+$ T_H cell

subsets. *In vitro*-polarized subsets were generated from naïve T_H cells (see Experimental Procedures), and include: ThN – non-polarized cells; Th1 cells; Th2 cells; induced T regulatory (iTreg) cells; NP-Th17 – non-pathogenic Th17 cells; P-Th17 – pathogenic Th17 cells. *Ex vivo* cells were FACS-sorted from spleen and peripheral lymph nodes using the gating strategy shown in Figure 1A: $Rh123^{hi}$ ($Mdr1^{-}$) or $Rh123^{lo}$ ($Mdr1^{+}$) effector T cells (Teff cells) or total Treg cells.

(B) Mean (x-axis) and differential (y-axis) gene expression, determined by RNA-seq., in $Rh123^{hi}$ ($Mdr1^{-}$) or $Rh123^{lo}$ ($Mdr1^{+}$) Teff cells FACS-sorted from mesenteric lymph nodes of FVB.*Rag1*$^{-/-}$ mice 6 weeks after wild type naïve T_H cell transfer. ATP-binding cassette (ABC) transporter genes are highlighted blue and annotated; *Abcb1a* (Mdr1a) is highlighted red.

(C) *Top*, FACS analysis of CD44 and hCD2 expression in Th17 fate-mapping reporter (*Il17a*$^{+/iCre}$ *R26*$^{+/LSL\text{-}hCD2}$) splenocytes following *ex vivo* stimulation with PMA and ionomycin. CD44/hCD2 expression is shown in live $CD3^{+}CD4^{+}CD25^{-}$ T conventional (Tconv) cells. Numbers indicate percentages of $CD44^{hi}hCD2^{-}$ (non-Th17, blue) and $CD44^{hi}CD2^{+}$ (Th17, red) Teff cells. *Bottom*, intracellular cytokine (IL-17A, IFNγ) expression in stimulated $CD44^{hi}hCD2^{-}$ (non-Th17) and $CD44^{hi}CD2^{+}$ (Th17) Teff cells. Representative of 3 mice. LSL, Lox-stop-Lox transcriptional termination cassette.

(D) *Top*, FACS analysis of CD44 and hCD2 expression in *ex vivo*-stimulated Tconv cells (gated as in **(C)**) isolated from spleen or colon lamina propria (cLP) of B6.*Rag1*$^{-/-}$ mice 6 weeks after wild type (B6) or Th17 fate-mapping reporter (*Il17a*$^{+/iCre}$ *R26*$^{+/LSL\text{-}hCD2}$) naïve T_H cell transfer. Numbers indicate percentages of $CD44^{hi}hCD2^{-}$ (non-Th17, blue) and $CD44^{hi}CD2^{+}$ (Th17, red) Teff cells. *Bottom*, intracellular cytokine (IL-17A, IFNγ) expression in stimulated $CD44^{hi}hCD2^{-}$ (non-Th17) and $CD44^{hi}CD2^{+}$ (Th17) Teff cells from transferred B6.*Rag1*$^{-/-}$ mice. Representative of 3 mice.

(E-F) *Ex vivo* FACS analysis of Mdr1-dependent Rh123 efflux (red peaks) in $hCD2^{-}$ (non-Th17, top) or $hCD2^{+}$ (Th17, bottom) Teff cells, gated as in **(C-D)**, from tissues of transferred B6.*Rag1*$^{-/-}$ 6 weeks after naïve T_H cell transfer as in **(D)**. *Ex vivo* Rh123 labeling and efflux was performed on resting/unstimulated cells; background Rh123 efflux is shown in elacridar-treated cells (shaded peaks). Numbers indicate percentages of $Rh123^{lo}$ ($Mdr1^{+}$) cells; representative of 3 mice. Representative raw data is shown in **(E)**; mean percentages of $Rh123^{lo}$ ($Mdr1^{+}$) cells (± SEM; n = 3) are shown in **(F)**. MLN, mesenteric lymph nodes; siLP, small intestine lamina propria; cLP, colon lamina propria.

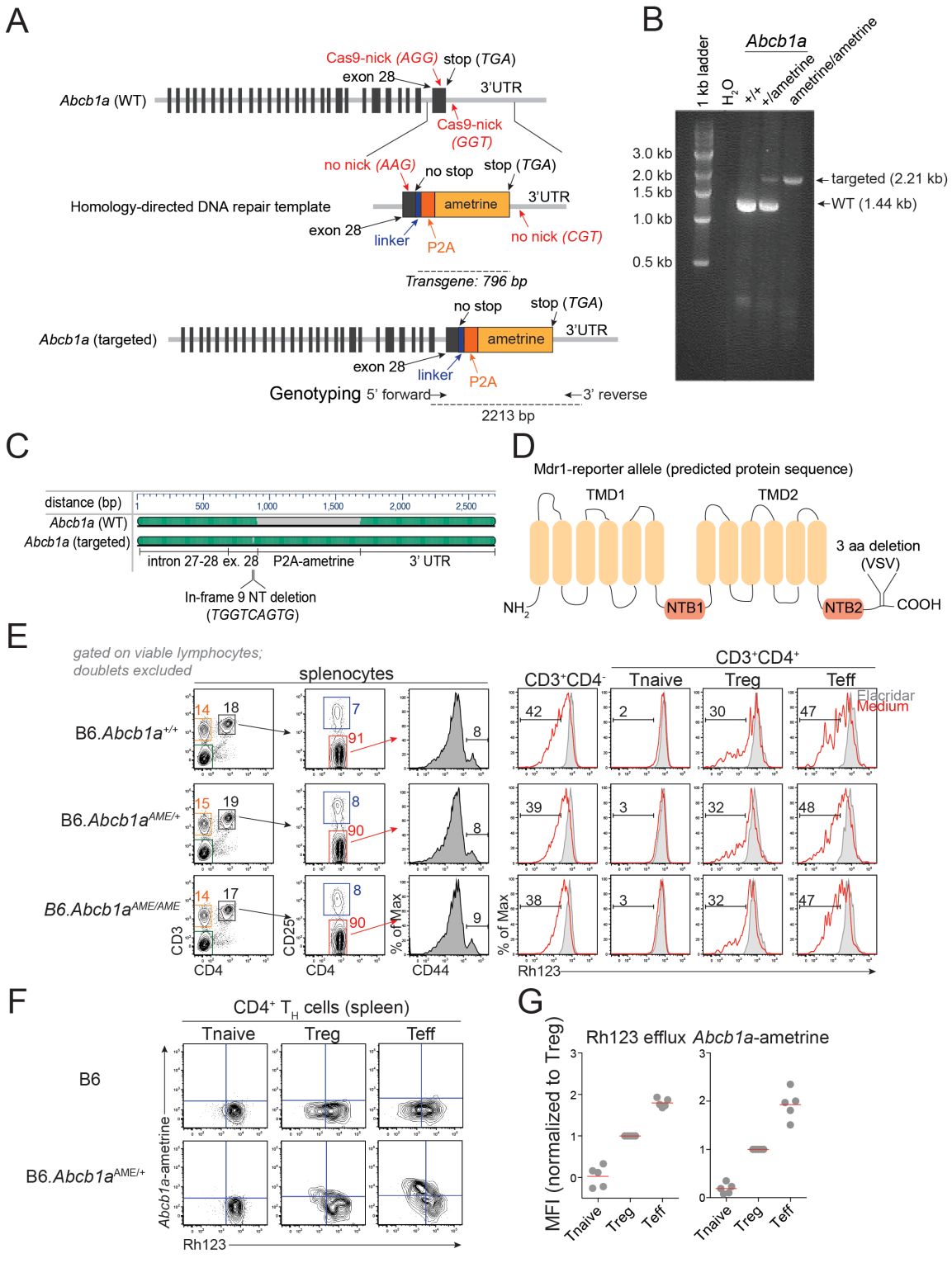

Figure S2. Generation of a Fluorescent Mdr1 Reporter Mouse (related to Figure 1).

(A) Schematic overview of the targeting strategy. *Top*, the wild type (WT) mouse *Abcb1a* locus (GenBank ID NM_011076.2). Black boxes indicate exons; black text/arrowhead indicate the stop codon and exon 28; red text/arrowheads indicate guide RNA-directed Cas9 cleavase (Cas9-nick) sites and protospacer adjacent motifs (PAMs; nGGs) proximal to the stop codon. *Middle*, the homology-directed DNA repair (HDR) template. Point mutations in the PAMs abolish Cas9 cleavase activity toward the HDR template, and are indicated by red text/arrowheads. Composition (Gly-Ser-Gly linker-P2A-ametrine) and size (796 bp) of the reporter transgene is shown. *Bottom*, the targeted *Abcb1a* allele. The location of genotyping primers, and size (2213 bp) of the amplified transgenic allele is shown (see Experimental Procedures for further details).

(B) Representative genotyping results from a wild type (B6; $Abcb1a^{+/+}$), heterozygous reporter ($Abcb1a^{AME/+}$), and homozygous reporter ($Abcb1a^{AME/AME}$) mouse. Sizes of the wild type and targeted PCR amplicons are shown at right; 1 kb ladder sizes are shown at left.

(C) Sequence alignment of the wild type (WT, GenBank ID NM_011076.2) and reporter *Abcb1a* alleles. Green indicates sequence identity; grey indicates dissimilarity. Position of introns, exons, the P2A-ametrine reporter transgene, and the 3' untranslated region (UTR) are indicated below. A functionally silent 9-nucleotide (NT) in-frame deletion (see **(E)** below) is present in the $Abcb1a^{ametrine}$ reporter allele near the upstream Cas9-nick site (shown in **(A)**).

(D) Schematic diagram of the predicted Mdr1a protein translated from the $Abcb1a^{ametrine}$ reporter allele. The in-frame 3 amino acid (aa) deletion near the non-conserved C-terminal end is shown. TMD, transmembrane domains 1 and 2; NTB, nucleotide-binding domains 1 and 2.

(E) *Ex vivo* FACS analysis of Rh123 efflux (red peaks) in splenic T cell subsets from wild type (B6.$Abcb1a^{+/+}$), heterozygous ($Abcb1a^{AME/+}$), and homozygous ($Abcb1a^{AME/AME}$) Mdr1-reporter mice. Gating strategies for, and frequencies of, T cell subsets are shown. Background Rh123 efflux is shown in elacridar-treated cells (shaded peaks). Representative of 3 experiments.

(F) Rh123 efflux as a function *Abcb1a*-ametrine expression in splenic Tnaive, Treg, and Teff cells (gated as in **(E)**) from wild type (B6; *top*), or Mdr1-heterozygous reporter ($Abcb1a^{+/ametrine}$; *bottom*) mice. Representative of 5 experiments.

(G) Normalized Rh123 efflux (*left*) or *Abcb1a*-ametrine expression (*right*) in splenic Tnaive, Treg, or Teff cells (gated as in **(E)**) from Mdr1-heterozygous reporter mice. Calculations of normalized Rh123 efflux and *Abcb1a*-ametrine expression are described in Experimental Procedures, and presented here relative to Treg cells. Horizontal red lines indicate mean values.

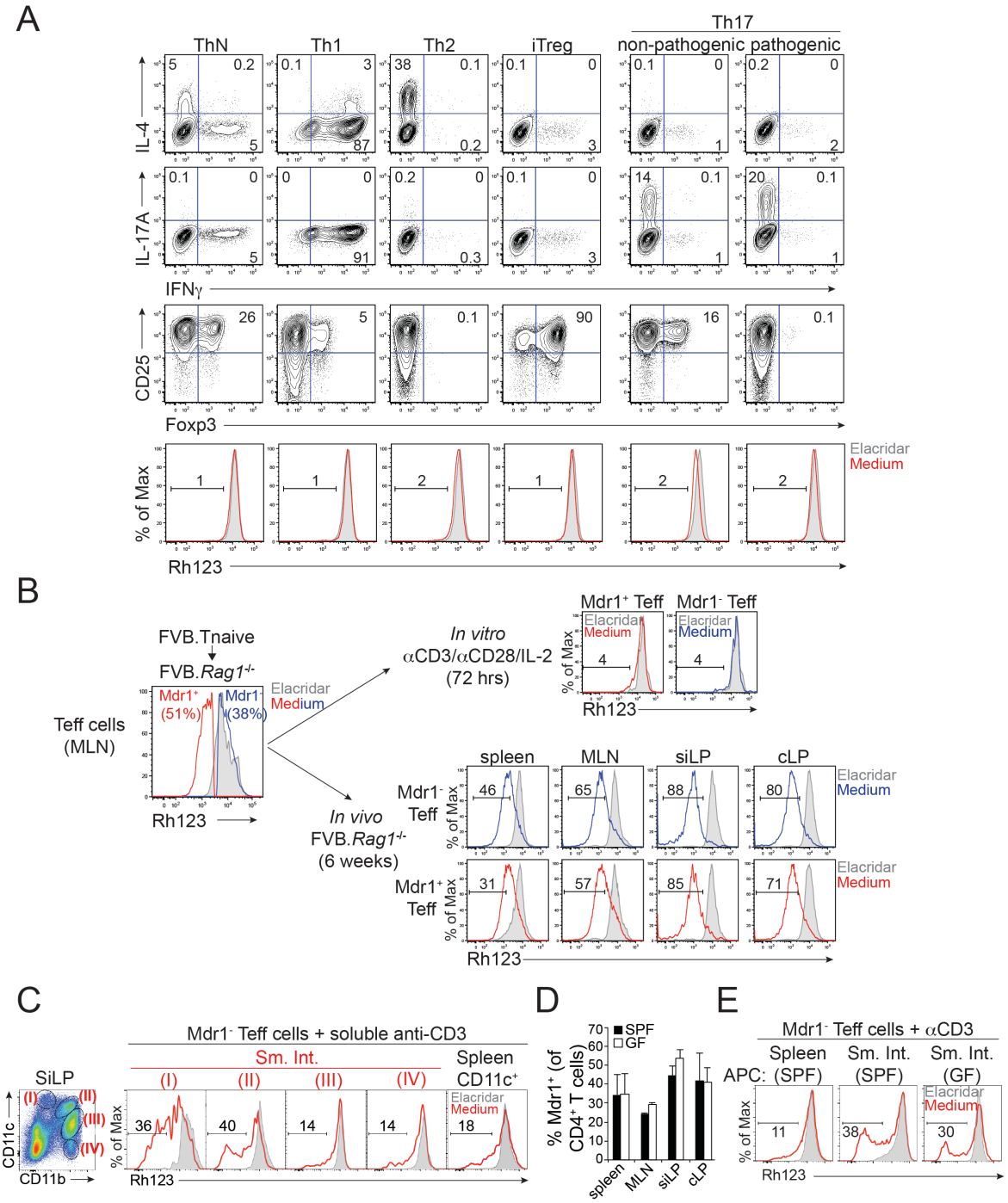

Figure S3. Mdr1 Expression in Effector T_H Cells is Transient and Induced by Intestinal Antigen-Presenting Cells (related to Figure 1).

(A) Intracellular cytokine expression (*top 2 rows*), surface CD25 and intracellular Foxp3 expression (*3rd row*), and Mdr1-dependent Rh123 efflux (*4th row*) in *in vitro*-differentiated wild type (B6) T_H cell subsets (subsets described in Figure S1A). Foxp3/CD25 expression was analyzed

on day 3 without re-stimulation; cytokine expression on day 4 (for iTreg and Th17 subsets) or day 5 (for ThN, Th1, and Th2 subsets) following re-stimulation with PMA/ionomycin. Rh123 efflux was measured on day 4 without re-stimulation; shaded peaks show background Rh123 efflux in elacridar-treated cells. Representative of 5 experiments.

(B) *Left*, FACS-sorting of *ex vivo* $Mdr1^+$ ($Rh123^{lo}$; red trace) or $Mdr1^-$ ($Rh123^{hi}$; blue trace) effector/memory T_H cells (Teff cells; gated as in Figure 1A) from mesenteric lymph nodes (MLN) of FVB.*Rag1*$^{-/-}$ mice 6 weeks after naïve T_H cell (Tnaive) transfer. *Top right*, Mdr1-dependent Rh123 efflux in FACS-sorted $Mdr1^+$ (red) or $Mdr1^-$ (blue) Teff cells (as above) 3 days after *in vitro* activation and expansion in the presence of anti-CD3/anti-CD28 beads recombinant IL-2. *Bottom right*, Mdr1-dependent Rh123 efflux in FACS-sorted $Mdr1^+$ (red) or $Mdr1^-$ (blue) Teff cells (as above) 6 weeks after re-transfer into naïve FVB.*Rag1*$^{-/-}$ mice. Background Rh123 efflux is shown throughout in elacridar-treated cells (shaded peak). siLP, small intestine lamina propria; cLP, colon lamina propria. Representative of 3 experiments.

(C) *Left* –Expression of CD11c and CD11b in siLP mononuclear cells from wild type (B6) mice. Red roman numerals indicate FACS-sorted subsets used in T cell co-culture experiments (below). *Right*, Rh123 efflux in ex *vivo*-sorted $Mdr1^-$ ($Rh123^{hi}$) Teff cells from siLP of wild type (B6) mice 4 days after *in vitro* stimulation with soluble anti-CD3 in the presence of FACS-sorted siLP or spleen antigen-presenting cell (APC) subsets (as above). Background Rh123 efflux is shown in elacridar-treated cells (shaded peak). Representative of 3 experiments.

(D) Mean percentages ($\pm$ SEM, n = 5-9) of $Rh123^{lo}$ ($Mdr1^+$) $CD4^+$ T_H cells, determined by *ex vivo* FACS analysis of Rh123 efflux, in tissues from wild type (BALB/c) mice maintained in specific pathogen-free (SPF) or germ free (GF) environments.

(E) Rh123 efflux in FACS-sorted wild type (BALB/c) $Mdr1^-$ Teff cells from siLP 4 days after *in vitro* stimulation with soluble anti-CD3 in the presence of FACS-sorted $CD11c^+$ APC from spleen or siLP of specific pathogen-free (SPF) or Sm. Int. of germ free (GF) BALB/c mice. Representative of 3 experiments.

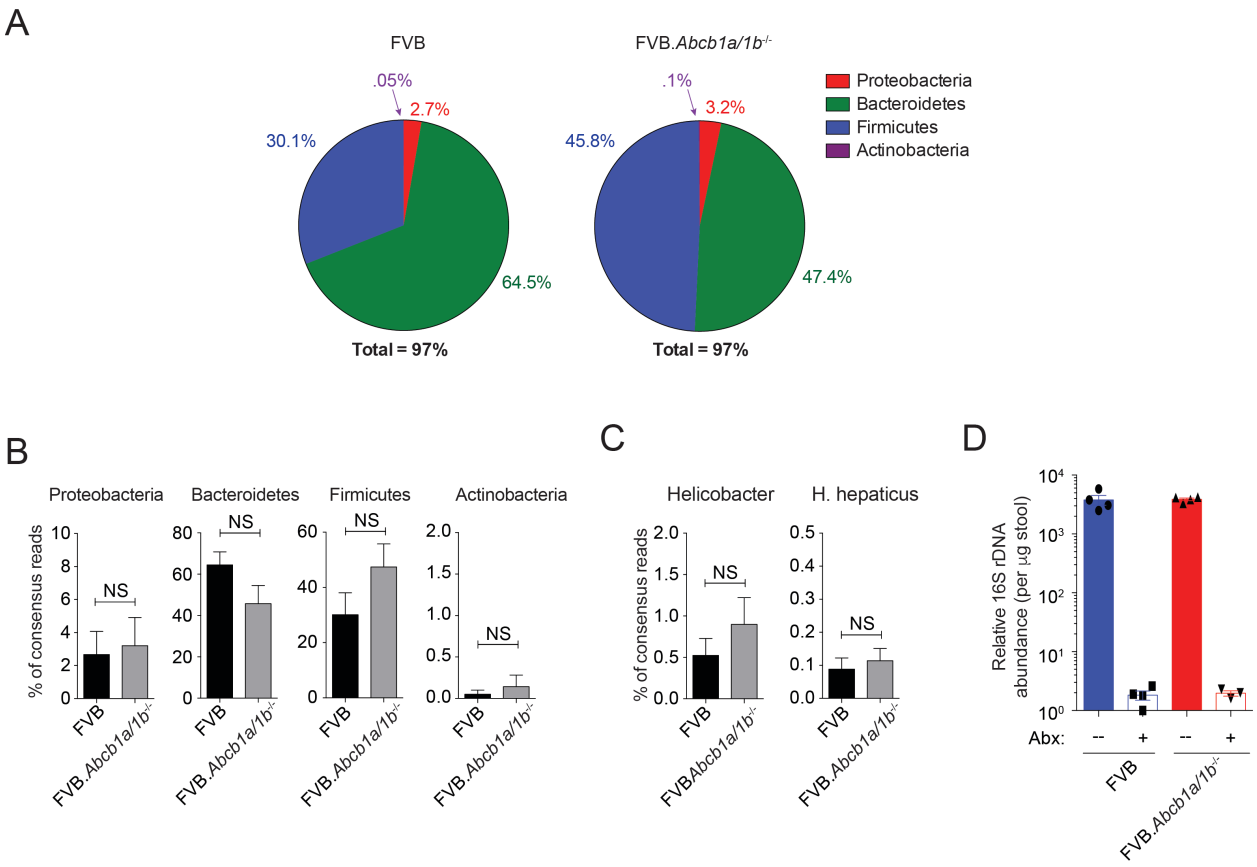

Figure S4. Ileitis Transferred by Mdr1-Deficient T_H Cells in *Rag1*$^{-/-}$ Hosts is not Associated with Dysbiosis (related to Figure 2).

(A) Cecal microbiome of untreated and co-housed FVB.*Rag1*$^{-/-}$ mice 6 weeks after receiving naïve T_H cells (Tnaive) from FVB wild type (*left*) or Mdr1-deficient (*Abcb1a/1b*$^{-/-}$, FVB.Mdr1ko; *right*) mice. Average percentages (n = 5) of phyla-specific relative to total consensus reads are shown. Determined by DNA sequencing (DNA-seq.) of *16S* ribosomal DNA (rDNA).

(B-C) Mean abundance (± SEM; n = 5) of major commensal phyla (proteobacteria, bacteroidetes, firmicutes, actinobacteria) **(B)** or total *Helicobacter* (*left*) or *Helicobacter hepaticus* (*H. hepaticus*, *right*) **(C)** in cecal stool of untreated, co-housed, and transferred FVB.*Rag1*$^{-/-}$ mice as in **(A)**. NS – not significant, student's t test.

(D) Mean relative abundance (± SEM; n = 3-4) of total bacterial DNA (*16S* rDNA) in cecal stool from co-housed FVB.*Rag1*$^{-/-}$ mice 6 weeks after receiving Tnaive cells from wild type (FVB) or Mdr1-deficent (FVB.Mdr1ko) mice, and treatment +/- antibiotics (Abx) as in Figure 2D. *16S* rDNA levels determined by qPCR.

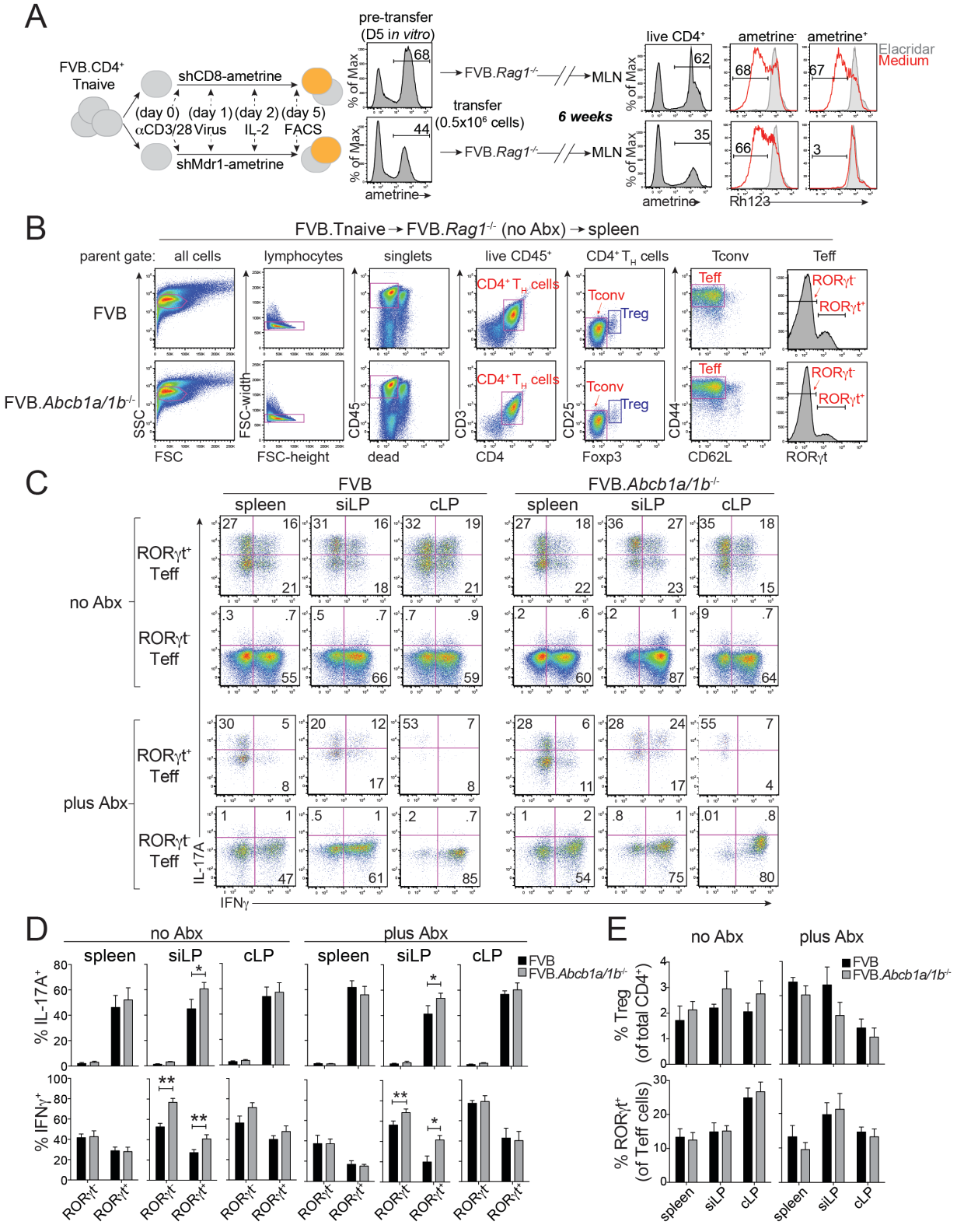

Figure S5. Mdr1 Selectively Regulates T Cell Cytokine Production in the Small Intestine (related to Figure 3).

(A) Anti-CD3/anti-CD28-stimulated wild type (FVB) $CD4^+$ naïve T_H (Tnaive) cells were transduced at 24 hr with ametrine-labeled retroviruses expressing control (*Cd8a*, shCD8) or Mdr1 (*Abcb1a* + *Abcb1b*, shMdr1) shRNAmirs. IL-2 was added to infected cells at day 2, and cells were expanded until day 5 post-activation. Transduction was confirmed by FACS analysis of ametrine expression, and unsorted cells were transferred into FVB.*Rag1*$^{-/-}$ mice. Mononuclear cells were re-isolated from mesenteric lymph nodes (MLN) 6 weeks-post transfer, and stable transduction in donor T_H cells was confirmed by *ex vivo* FACS analysis. Mdr1 knockdown was assessed by FACS analysis of Rh123 efflux in ametrine$^+$ and ametrine$^-$ donor T_H cells. Background Rh123 efflux is shown in elacridar-treated cells (shaded peaks). Representative of 3 experiments.

(B) Gating strategy used to discriminate total and RORγt+/- Teff cells from tissues of transferred *Rag1*$^{-/-}$ mice. Representative data are shown from spleen mononuclear cells recovered from untreated (no antibiotics [Abx]) FVB.*Rag1*$^{-/-}$ mice 6 after receiving Tnaive cells from wild type (FVB, *top*) or Mdr1-deficient (Mdr1ko; *Abcb1a/1b*$^{-/-}$, *bottom*) mice. Red/blue text indicates populations of interest. Representative of more than 20 mice.

(C) IL-17A and IFNγ expression in *ex vivo*-stimulated wild type (FVB) or FVB.Mdr1ko RORγ +/- Teff cells (gated as in **(B)**) from tissues of untreated (no Abx, *top*) or antibiotic-treated (plus Abx, *bottom*) transferred FVB.*Rag1*$^{-/-}$ mice. Analysis was performed 6 weeks-post Tnaive cell transfer. Numbers indicate percentages of cytokine-positive cells; representative of 6 mice analyzed in 3 independent experiments. siLP, small intestine lamina propria; cLP, colon lamina propria.

(D) Mean percentages (± SEM; $n = 6$) of IL-17A- (*top*) or IFNγ (*bottom*)-expressing wild type (FVB) or FVB.Mdr1ko RORγt+/- Teff cells from tissues of untreated (no Abx, *left*) or antibiotic-treated (plus Abx, *right*) transferred FVB.*Rag1*$^{-/-}$ mice as in **(C)**.

(E) Mean percentages (± SEM; $n = 6$) of wild type (FVB) or FVB.Mdr1ko Treg (*top*) or RORγ$^+$ Teff (*bottom*) cells from tissues of untreated (no Abx, *left*) or antibiotic-treated (plus Abx, *right*) transferred FVB.*Rag1*$^{-/-}$ mice as in **(B)**.

* $P < .05$, ** $P < .01$, student's *t* test.

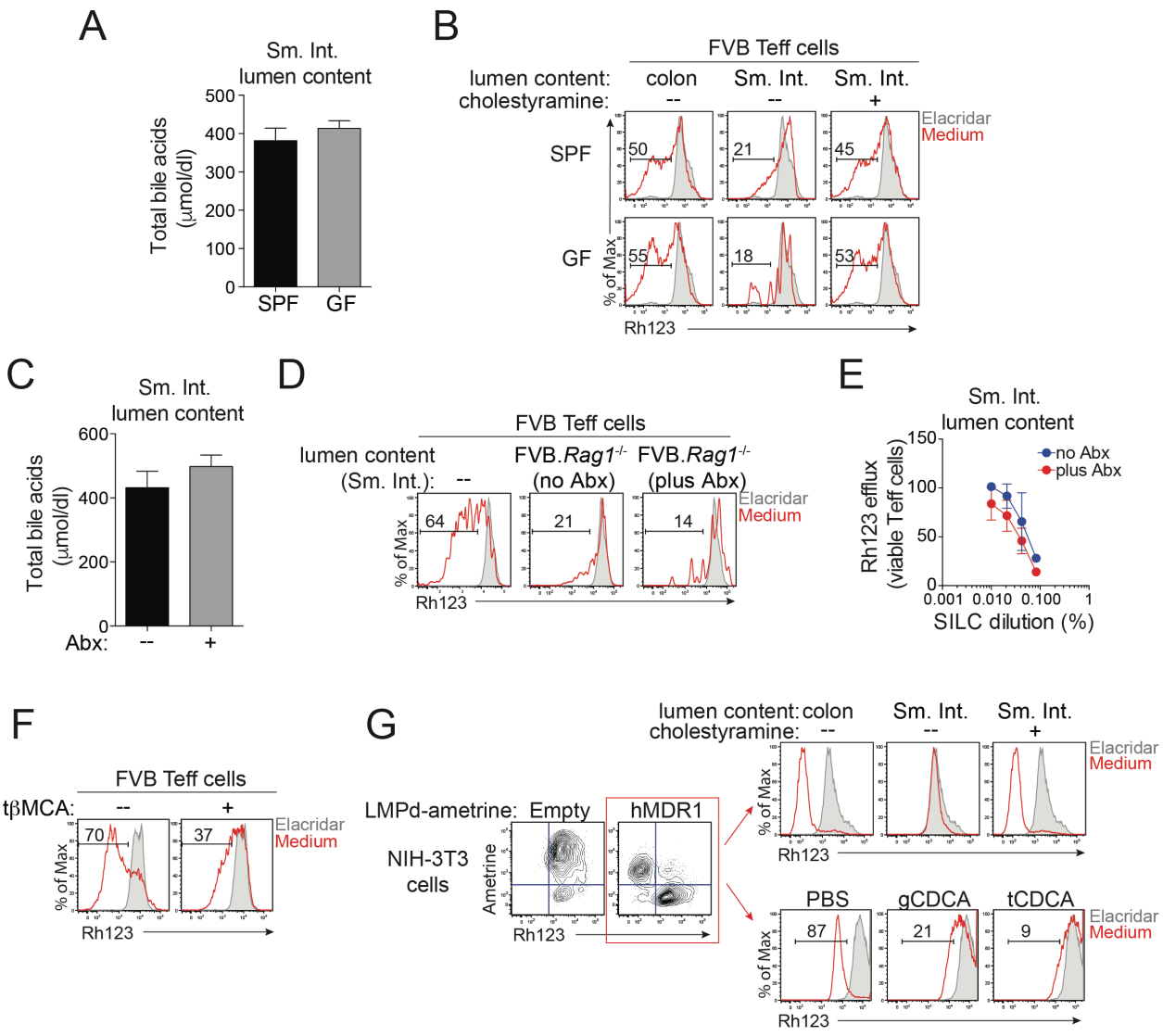

Figure S6. Interplay Between Mdr1 and Intestinal Bile Acids (related to Figure 4).

(A) Mean bile acid concentrations (± SEM; $n = 10$) in small intestine lumen contents from specific pathogen-free (SPF) or germ free (GF) wild type BALB/c mice.

(B) FACS analysis of Mdr1-dependent Rh123 efflux in splenic wild type (FVB) $CD4^+$ effector/memory T cells (Teff cells; gated as in Figure 1A) after *ex vivo* treatment of whole splenocytes with sterile, soluble lumen content from colon or small intestine (Sm. Int.) of SPF or GF wild type BALB/c mice. Background Rh123 efflux is shown in elacridar-treated cells (shaded peaks). Sm. Int. lumen contents were pre-treated +/- cholestyramine to deplete bile acids (as in Figure 4A; see also Experimental Procedures). Representative of 3 experiments.

(C) Mean bile acid concentrations (± SEM; n = 4) in Sm. Int. lumen content from FVB.*Rag1*$^{-/-}$ mice after receiving wild type (FVB) CD4^{+} naïve T_H (Tnaive) cells and treatment +/- antibiotics (Abx) as in Figure 2D-F.

(D) FACS analysis of Mdr1-dependent Rh123 efflux in wild type (FVB) splenic Teff cells (gated as in Figure 1A) after *ex vivo* treatment of whole splenocytes +/- Sm. Int. lumen content from FVB.*Rag1*$^{-/-}$ mice after receiving wild type (FVB) Tnaive cells and treatment +/- antibiotics (Abx) as in Figure 2D-F; background Rh123 efflux is shown in elacridar-treated cells (shaded peaks). Representative of 3 experiments.

(E) Dose-response of Sm. Int. lumen content from transferred FVB.*Rag1*$^{-/-}$ mice treated +/- antibiotics (Abx) on Mdr1-dependent Rh123 efflux in wild type (FVB) splenic Teff cells as in **(D)**. Mean Rh123 efflux activity (± SEM; n =3) is normalized to vehicle (PBS)-treated Teff cells.

(F) FACS analysis of Mdr1-dependent Rh123 efflux in wild type (FVB) Teff cells after *ex vivo* treatment of whole splenocytes +/- tauro-β-muricholate (tβMCA; 2.5 mM); background Rh123 efflux is shown in elacridar-treated cells (shaded peaks). Representative of 3 experiments.

(G) *Left*, FACS analysis of Rh123 efflux in Mdr1^{-} NIH-3T3 mouse embryonic fibroblasts transduced with empty or wild type human MDR1 (hMDR1)-expressing ametrine retroviruses (LMPd). *Top right*, Rh123 efflux in hMDR1-expressing NIH-3T3 cells (gated as ametrine^{+}) after treatment +/- Sm. Int. lumen content from wild type (FVB) mice treated +/- cholestyramine as in **(B)**. *Bottom right*, Rh123 efflux in hMDR1-expressing NIH-3T3 cells (gated as ametrine^{+}) after treatment with vehicle (PBS), or glycine (g)- or taurine (t)-conjugated chenodeoxycholic acid (CDCA) (1.2 mM). Background Rh123 efflux is shown in elacridar-treated cells. Representative of 3 experiments.

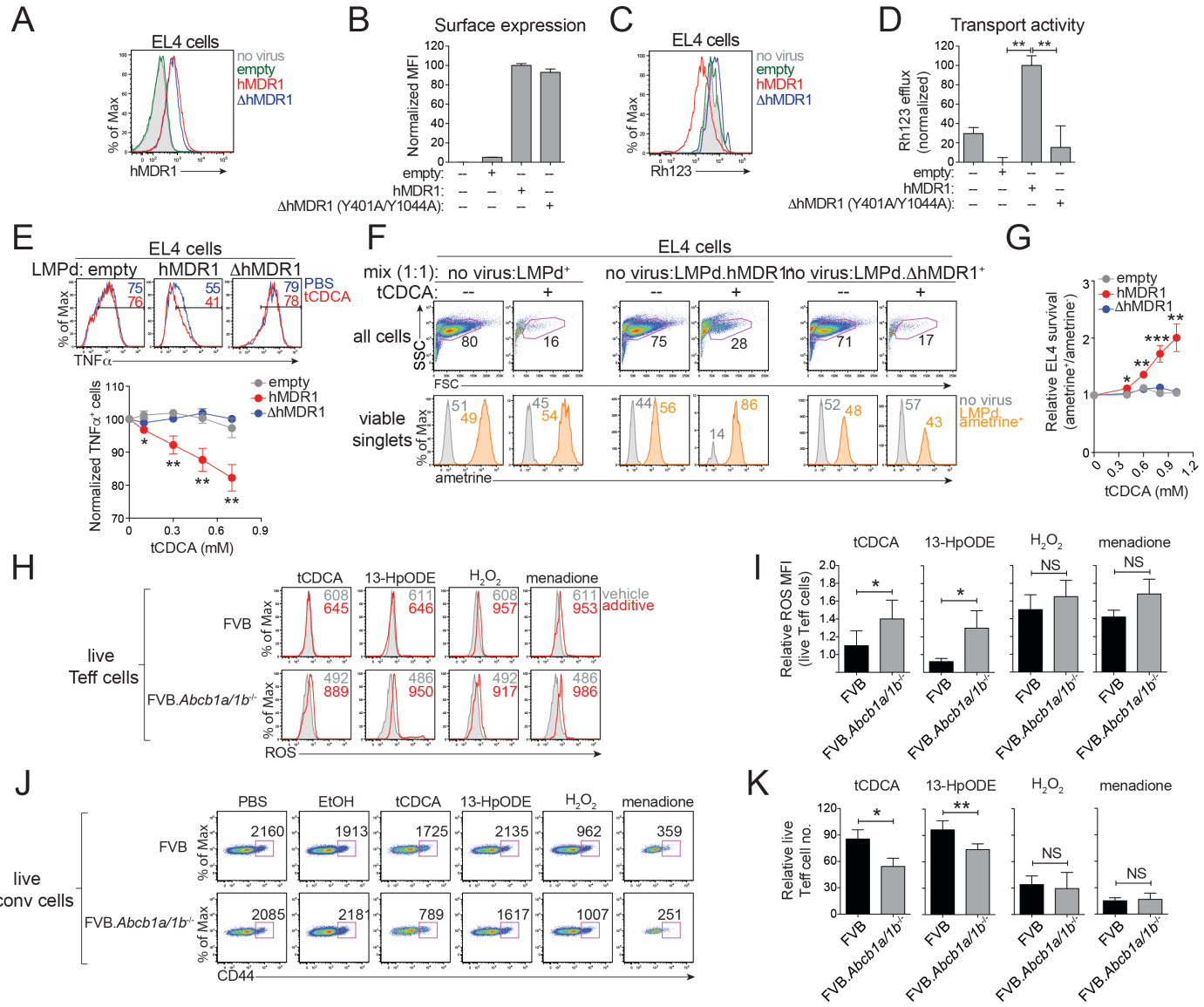

Figure S7. MDR1 Regulates Effector T Cell Homeostasis in the Presence of Conjugated Bile Acids (related to Figures 4-5).

(A) FACS analysis of human MDR1 cell surface expression in Mdr1$^-$ mouse EL4 lymphoma cells left untransduced (no virus; shaded), or transduced with empty (green), wild type human MDR1 (hMDR1; red)- or transport-deficient mutant hMDR1 (ΔhMDR1; Y401A/Y1044A)-expressing ametrine retroviruses. Expression is shown in ametrine$^-$ (no virus) or ametrine$^+$ (transduced) gated cells. Representative of 3 experiments.

(B) Mean normalized surface MDR1 mean fluorescent intensity (MFI) (± SEM; n = 3) in EL4 cells left untransduced or transduced as in **(A)**.

(C) FACS analysis of Mdr1-dependent Rh123 efflux in EL4 cells left untransduced or transduced as in **(A)**. Rh123 efflux is shown in ametrine$^-$ (no virus) or ametrine$^+$ (transduced) gated cells. Representative of 3 experiments.

(D) Mean normalized Rh123 efflux (± SEM; n = 3) in EL4 cells left untransduced or transduced as in (**A**), and determined by FACS analysis as in **(C)**.

(E) *Top*, TNFα expression in EL4 cells transduced with empty, wild type hMDR1-expressing, or transport-deficient ΔhMDR1-expressing retroviruses as in **(A)** after PMA/ionomycin stimulation. Representative of 4 experiments. *Bottom*, dose responses of taurine-conjugated chenodeoxycholic acid (tCDCA) on TNFα expression (± SEM; n = 4-8) in PMA/ionomycin-stimulated EL4 cells transduced with empty, wild type hMDR1-expressing, or transport-deficient ΔhMDR1-expressing retroviruses as above. Percentages of TNFα$^+$ cells are normalized to vehicle (PBS)-treated cells.

(F) Untranduced EL4 cells (no virus) were mixed (1:1) with FACS-sorted transduced (ametrine$^+$) EL4 cells expressing nothing (empty), wild type (hMDR1), or transport-deficient mutant (ΔhMDR1) human MDR1; these congenic mixtures were then treated overnight +/- tCDCA (1.2 mM). Surviving lymphocytes, based on forward/side scatter (FSC/SSC; *top*), and percentages of viable ametrine$^-$ (no virus; grey) and ametrine$^+$ (transduced) cells (*bottom*) are shown. Representative of 5 experiments.

(G) Mean relative survival (± SEM; n = 5-8) of transduced EL4 cells expressing nothing (empty), wild type (hMDR1), or transport-deficient mutant (ΔhMDR1) human MDR1 after overnight treatment +/- tCDCA as in **(F)**. Transduced (ametrine$^+$) EL4 cell survival is shown relative to co-cultured untransduced (ametrine$^-$) EL4 cells.

(H) Reactive oxygen species (ROS) levels, determined by flow cytometry, in wild type (FVB; *top*) or FVB.Mdr1ko (*bottom*) splenic CD4$^+$ effector/memory (Teff) cells (gated as in Figure 1A) 8 hr after treatment of whole splenocytes with vehicle controls (PBS, EtOH; shaded peaks), tCDCA

(1.2 mM), 13-hydroperoxy-octadecadienoic acid (13-HpODE; 50 μM), hydrogen peroxide (H_2O_2; 0.5 mM), or menadione (15 μM) (red peaks). Numbers indicate ROS mean fluorescence intensities (MFIs). Representative of 3-6 experiments.

(I) Mean relative MFIs of ROS staining (± SEM) in wild type (FVB) or FVB.Mdr1ko Teff cells after treatment with tCDCA ($n = 6$), 13-HpODE ($n = 6$), H_2O_2 ($n = 3$), or menadione ($n = 5$) as in **(H)**. ROS levels are normalized to the appropriate vehicle control (PBS for tCDCA and H_2O_2; EtOH for 13-HpODE and menadione).

(J) Survival of $CD44^{hi}$ Teff cells within wild type (FVB; *top*) or FVB.Mdr1ko (*bottom*) splenocytes after 8 hr treatment with vehicle controls (PBS, EtOH), tCDCA, 13-HpODE, H_2O_2, or menadione as in **(H)**. CD44 staining is shown in live (viability dye^-) $CD4^+CD25^-$ (Tconv) cells; relative cell numbers determined by flow cytometry are indicated. Data represent 3-6 experiments.

(K) Mean relative live Teff cell numbers (± SEM) after 8 hr treatment of wild type (FVB) or FVB.Mdr1ko splenocytes +/- tCDCA ($n = 6$), 13-HpODE ($n = 6$), H_2O_2 ($n = 3$), or menadione ($n = 5$) as in **(H, J)**. Live Teff cell numbers are normalized to the appropriate vehicle control (PBS for tCDCA and H_2O_2, EtOH for 13-HpODE and menadione).

* $P < .05$, ** $P < .01$, *** $P < .001$, student's *t* test.

SUPPLEMENTAL TABLES

	Healthy controls	Ulcerative colitis	Crohn's disease (No Ileitis)	Crohn's disease (Ileitis)
Number	58	58	29	38
Age range	21-67	22-72	21-88	20-82
mean ± SD	41.33 ± 13.31	39.32 ± 14.09	38.07 ± 16.11	41.00 ± 15.23
Not Provided	3	0	2	1
Gender male	22	33	17	20
female	34	25	11	18
Not Provided	2	0	1	
Ethnicity Caucasian	13	40	20	26
Hispanic	3	2	1	7
African	1	1	0	2
Asian	0	2	2	1
Other minority	1	10	3	1
Not Provided	40	3	3	1

Table S1. Demographic Data of the Healthy Volunteer and IBD Patient cohorts (related to Figure 7).